energies

MDPI

Article

Smart Reuse of Waste Heat from Data Centres: Energy and Exergy Analysis for a District-Heating Network in Bulgaria

Antonio Verzino, Lorenzo Talluri, Andrea Rocchetti * and Luca Socci *

Thermodynamics and Heat Transfer Research Group, c/o Department of Industrial Engineering, University of Florence, 50139 Firenze, Italy; antonio.verzino@unifi.it (A.V.); lorenzo.talluri@unifi.it (L.T.)
* Correspondence: andrea.rocchetti@unifi.it (A.R.); luca.socci@unifi.it (L.S.)

Abstract

The rapid growth of data centres is driving higher electricity consumption and continuous generation of low-grade waste heat. Integrating this heat into district-heating networks offers a smart strategy for thermal management in urban areas. In this context, this study presents an energy and exergy analysis of an integrated system comprising a data centre, vapour-compression heat pumps, thermochemical energy storage, and a third-generation district-heating network in Varna (Bulgaria). The proposed system relies on data-centre waste-heat recovery via vapour-compression heat pumps and thermochemical energy storage, enabling seasonal decoupling between heat availability and demand. Despite the relatively small size of the data centre (500 kW) compared to the district-heating system (average thermal demand of 9.3 MW), recovered waste heat can supply up to 3.0% of the annual heat demand and over 20% of the instantaneous load. The integrated configuration consistently improves overall exergy efficiency, confirming its thermodynamic advantage. These findings show that data centres can act as reliable thermal assets for existing district-heating networks, with heat pumps and thermal energy storage emerging as key enablers for district-heating decarbonisation.

Keywords: data-centre waste-heat recovery; district-heating networks; heat pumps; thermochemical energy storage; energy and exergy analysis

1. Introduction

1.1. The Heating Sector: Current Situation and Perspectives of Decarbonisation

The heating and cooling sector accounts for around half of the final energy consumption in Europe: its decarbonisation is a central pillar of the European Union's climate ambitions. The *Recast Energy Efficiency Directive* (Directive EU 2023/1791) places new emphasis on energy efficiency and a substantial expansion in the utilisation of renewable and waste-heat sources [1]. In parallel, the *REPowerEU Plan* and the revision of the *Renewable Energy Directive* reinforce the need to deploy clean heating technologies at scale, highlighting district heating as a strategic technology [2]. According to the International Energy Agency, clean heating technologies, like heat pumps coupled with low-temperature networks, are indispensable for achieving net-zero pathways [3,4]. Similarly, the International Renewable Energy Agency identifies district-heating networks as an increasingly prominent technology in connecting local renewable and waste-heat sources to consumers [5]. Modern district heating and cooling systems offer a technically and economically

Academic Editor: Andres Siirde

Received: 2 January 2026
Revised: 30 January 2026
Accepted: 31 January 2026
Published: 3 February 2026

Copyright: © 2026 by the authors. Licensee MDPI, Basel, Switzerland. This article is an open access article distributed under the terms and conditions of the Creative Commons Attribution (CC BY) license.

robust pathway to reduce emissions from buildings and industry. More than 43% of district-heating supply already derives from renewable and waste heat, and the sector has the potential to expand significantly [6]. Large-scale heat pumps, in particular, are recognised as a cornerstone technology as they enable the harvesting of diverse low-temperature heat sources while providing operational flexibility when coupled with storage [6,7]. The growing penetration of low-temperature district-heating networks, together with the rise in urban waste-heat sources and the electrification of heating, creates favourable conditions for the integration of these low-grade thermal sources (such as data centres) into district-heating systems.

The following paragraphs describe the technological and systemic framework enabling the integration of data-centre waste heat into district-heating networks.

1.2. The District Heating Sector: Evolution and Future Trends

District Heating Networks (DHNs) are recognised as a key technology for the decarbonisation of the urban heating sector due to their ability to aggregate thermal demand and integrate renewable energy sources and multiple forms of waste heat [8,9]. DHNs have evolved through four main generations, characterised by a progressive reduction in operating temperatures, improvements in distribution efficiency, and a larger contribution of non-fossil heat sources [10,11]. Early generations operated at temperatures above 100 °C; third-generation networks introduced more efficient hot-water distribution systems, enabling the integration of industrial waste heat; the transition towards the fourth generation is based on further reductions in the temperatures, typically 50–60 °C for supply and 25–35 °C for return, facilitating the integration of renewable heat sources, low-temperature waste heat, and heat pumps [11–14]. In recent years, the concept of fifth-generation district heating and cooling has emerged based on near-ambient-temperature networks, allowing users to act as thermal prosumers [15,16]. The decarbonisation of district heating requires not only reductions in operating temperatures but also the development of more flexible networks capable of integrating distributed energy resources. Recent studies show that demand–response strategies, centralised heat pumps, and thermal energy storage can improve overall system efficiency and increase the utilisation of renewable and waste-heat sources [17–19]. When integrating renewable energy sources or waste heat, reducing operating temperatures is not always feasible, particularly for old, existing DHNs. Given this background, the present study analyses the integration of waste heat recovered from a data centre into a real district-heating system (third-generation), using the network of the city of Varna (Bulgaria) as a representative case study of current DHN conditions.

1.3. Data Centres as Emerging Sources of Waste Heat for District Heating

In the past two decades, the data-centre sector has experienced extremely rapid growth in the number of installations, computing capacity, and rack power density. This expansion has been driven by the rising demand for digital services, cloud computing, big data applications, and artificial intelligence. As a result, electrical consumption has increased significantly. Current estimates attribute between 1% and 2% of global electricity use to data centres, with a continuing annual rise [20–23]. Modern high-density servers can reach high thermal design power values, with rack powers often exceeding 20–30 kW and potentially reaching 50 kW per rack in future scenarios [24]. The demand for electricity for data centres is projected to more than double by 2030, reaching around 945 TWh per year, roughly equivalent to the current annual electricity consumption of a large industrialised country like Japan [25]. Recent projections indicate that the electricity demand of data centres could double, with a projected Compound Annual Growth Rate of around 14–15% up to 2030 [26,27]. These numbers underscore the rapidly expanding energy

footprint of data centres and highlight the importance of efficient energy-management strategies. The combination of increasing loads, continuous 24/7 operation, and high equipment concentration leads to a substantial rise in cooling demand, considering that the fundamental characteristic of data centres is the conversion of electrical input into heat, with a ratio of 1:1. Multiple studies indicate that cooling systems can account for up to 40–50% of total data-centre energy consumption if thermal management is inefficient [23,28–30].

The increasing cooling demand results not only in a higher overall electrical load, but also in greater availability of low-temperature waste heat. Heat dissipated by the cooling system is a thermal resource that is currently underutilised. Growing interest in energy efficiency and decarbonisation approaches is encouraging the view of data centres not only as energy-consuming nodes and contributors to the "urban heat island effect", but as potential thermal sources. Depending on the cooling technology, the temperature of the recoverable heat typically ranges between 25 and 35 °C (or higher) in air-based systems and between 50 and 60 °C in liquid-cooling configurations [31,32]. These temperature levels could be integrated in third-generation district-heating systems, provided that an adequate thermal upgrade (e.g., via heat pumps) is implemented [33], and they are well-suited for low-temperature district-heating networks, such as fourth- and fifth-generation district heating [34]. Waste-heat recovery from data centres can be achieved through different strategies: direct heat exchange via heat exchangers, integration with heat pumps for temperature upgrading, or hybrid configurations combining both. Booster heat pumps and pinch-based thermal analyses allow maximisation of recoverable heat and improve the matching between source and demand temperatures [35]. The literature clearly highlights that integrating data-centre waste heat into district-heating networks can reduce fossil-fuel consumption, increase system flexibility, and improve overall thermal-production efficiency. Urban- and national-scale assessments indicate that systematic utilisation of waste heat can reduce DHN operating costs by 0.6–7.3% [36] and lower total system emissions by 1–2% in mid-term scenarios [37]. The continuous availability of the thermal stream is a key advantage as it can reliably cover base-load or mid-load thermal demands [38]. Multiple case studies confirm the high reliability of heat recovered from data centres. Real-world implementations in Europe and China demonstrate the effectiveness of DC → HP → DHN configurations, achieving measurable energy savings and significant increases in system efficiency [31,39].

Overall, the available evidence supports the view that data centres can evolve from purely energy-intensive electrical loads into active thermal nodes within urban energy systems, contributing to emission reductions, improved energy efficiency, and the valorisation of digital infrastructure in the context of low-temperature district heating.

1.4. Heat-Pump Technology: State of the Art and Perspectives

Heat pumps (HPs) are a well-established technology widely employed for upgrading low-temperature heat sources, including waste heat released by data centres. Vapour-compression heat pumps, nowadays the most diffuse, may be classified into categories according to their supply temperatures: low-temperature heat pumps (LTHPs), up to approximately 60 °C; medium-temperature heat pumps (MTHPs), 60–100 °C; high-temperature heat pumps (HTHPs), 100–160 °C; ultra-high-temperature heat pumps (UHTHPs), 160–200 °C [40]. For industrial and district-heating applications, HTHPs are of particular interest. Single-stage units are suitable for moderate temperature lifts (≤30–40 °C), whereas higher delivery temperatures require two-stage cycles, economiser configurations, vapour injection, or cascade systems using multiple refrigerants [41].

A key aspect for the advancement of high-temperature heat pumps is the selection of the fluid, involving considerations of thermodynamic efficiency, environmental impact

(fluids with zero ODP, negligible GWP, and no PFAS), and human safety [42]. Low-GWP refrigerants, such as ammonia (R717), hydrocarbons (R290 and R600), CO_2 (R744), and several HFO/HCFO compounds, exhibit favourable thermodynamic properties and are well-suited for medium- and high-temperature applications [40].

Heat pumps also play a central role in the transition of district-heating networks towards low-temperature operation, characterised by increasing integration of renewable energy sources and waste heat. The reductions in supply and return temperatures in modern district-heating networks improve efficiency, reduce distribution losses, and expand the range of exploitable heat sources, making heat pumps an enabling technology for modern district-heating systems [43,44]. Heat pumps can be deployed in centralised configurations, where large-scale units provide base-load heat with COP values 3–5 for supply temperatures up to 70–80 °C, or in decentralised configurations using booster heat pumps at the building level to support lower network temperatures and facilitate the transition from third- to fourth-generation systems [45]. In DHNs with a supply temperature in the range of 55–70 °C, centralised heat pumps can supply most of the thermal demand and reduce reliance on peak-load boilers. In DHNs with a supply temperature in the range of 35–50 °C, the combined operation of central heat pumps and decentralised booster units enables high overall efficiency, significant reductions in network losses, and improved exergetic quality of heat supply [13,46]. From both energy and exergy perspectives, the integration of heat pumps into district-heating systems offers multiple benefits. Lower network temperatures increase the COP and enhance the share of renewable and waste heat that can be utilised, while reduced temperature differences between source and sink decrease irreversibilities and improve overall system efficiency [47,48]. Evidence from European district-heating projects confirms that large-scale heat pumps are a mature and widely deployed technology, capable of maintaining high performance even under substantial temperature lifts [44].

1.5. Thermal Energy Storage for Flexible District-Heating Systems

Thermal Energy Storage (TES) technologies play a central role in modern energy systems as they enable the temporal decoupling of heat production and demand and improve overall operational flexibility.

TES solutions are commonly classified into three main categories: sensible heat storage (SHS), latent heat storage (LHS), and thermochemical storage (TCS) [49]. SHS technologies represent the most established option, relying on temperature variations in a liquid or solid medium. LHS systems employ phase-change materials (PCMs) to provide higher energy density and near-isothermal charge and discharge. Among emerging technologies, thermochemical storage (TCS) based on thermochemical materials (TCMs) has attracted increasing attention because of its high energy density, the absence of thermal losses during the storage period, and the possibility of long-term and seasonal operation [50,51].

TCS systems rely on reversible chemical or sorption reactions, where energy is stored in the bonding state of the reactants during charging and released during recombination. TCMs include zeolites, silica gel, salt hydrates, and composite structures combining porous matrices with reactive salts [52]. The high energy density and loss-free storage capability of TCS systems make them particularly suitable for applications where the availability of waste heat does not match the demand profile, or where seasonal storage is required. In particular, thermochemical materials can store low-grade heat and release it at controlled temperature levels, creating opportunities for integration within energy-intensive processes or coupled heat pump–district heating configurations.

In summary, while SHS and LHS provide mature and widely deployed solutions, TCS technologies offer a promising pathway for high-density, long-duration storage and

for enhancing the utilisation of waste-heat sources. Their potential role in advanced energy architectures motivates growing interest in their application within integrated energy systems. In particular, the increasing deployment of fourth- and fifth-generation district-heating networks, characterised by reduced operating temperatures and growing integration of renewable and waste-heat sources, makes TCS—and all thermal energy-storage methods in general—a strategic component for enhancing operational flexibility in the context of districtheating networks [53,54]. Short-term TES can reduce peak loads and enable heat-pump operation during favourable tariff periods, while seasonal storage enables extensive utilisation of waste heat and renewable energy even during high-demand periods. Integrated TES + demand–side management (DSM) systems further reduce operational costs and the required production capacity [55]. Recent studies indicate that thermochemical storage may be suitable for district-heating applications, particularly in networks with high full-load hours or substantial base-load needs [56].

Overall, thermal energy storage represents an essential component of modern district-heating networks: the interaction between heat pumps, waste-heat sources, and TES technologies—including emerging thermochemical solutions—opens new opportunities for integrated energy utilisation and enhanced recovery of waste heat, such as that analysed in the present study.

1.6. Novelty and Contributions of the Present Study

Despite the extensive scientific interest in district heating evolution, heat-pump integration, and data-centre waste-heat recovery, there is still a lack of studies assessing—on a real network and through a combined energy and exergy perspective—the full chain DC → HP → TES → DHN under realistic operating conditions. Furthermore, only a limited number of studies apply such methodologies to actual DHNs with measured heat-demand profiles, reducing the ability to evaluate practical system-level impacts.

The present study addresses this gap by developing an integrated energy–exergy assessment of a waste-heat recovery configuration for data centres coupled with a heat pump and thermal storage system, applied to the real district-heating network of the city of Varna (Bulgaria), which will be the central real case study of the Horizon Project THUNDER—*THermochemical storage Utilization eNabling Data centre seasonal Energy Recovery* [57]. This work extends the Authors' previous research on waste-heat recovery from DCs and reuse in third-generation DHNs [33], focused on a direct integration via heat pumps without long-term thermal storage. Compared to the earlier study, this manuscript introduces a thermochemical storage system enabling seasonal heat shifting, includes exergy analysis, and applies the methodology to a different, real district-heating network. These additions allow a deeper assessment of the thermodynamic performance and flexibility potential of data-centre integration in existing district-heating systems.

2. Materials and Methods

This chapter contains a description of the functioning and the modelling of the two compared scenarios.

In the first, referred to as *Scenario S0*, there is a traditional setup in which no integration of DC waste heat into the DHN occurs. The DC is, thus, traditionally cooled (indirect air-side free cooling, FC and active cooling, AC, by Vapour Compression Cycle, VCC), releasing the heat into the environment, while the thermal demand of the network is entirely met by its generation system based on fossil fuels (boiler). S0 serves as the baseline for comparing the results of waste-heat integration: yearly energy consumption for the autonomous cooling system, the amount of heat released into the environment, and the energy consumption for the DHN generation system were calculated to provide a comparison with the subsequent scenario. In the second scenario, referred to as *Scenario S1*,

the same DC releases its waste heat into the DHN through a thermochemical storage: the recovery is activated when the active cooling is on.

For both scenarios, two cases were evaluated: *Case A* with temperatures of inlet–outlet air of the data centre at 20–35 °C (maximum outdoor air temperature for free cooling at 15 °C); and *Case B* with temperatures of inlet–outlet air of the data centre at 25–40 °C (maximum outdoor air temperature for free cooling at 20 °C). Operation is assumed, for all scenarios and cases, with a data-centre air-distribution system based on a "hot aisle–cold aisle" configuration: this layout enables higher operating temperatures, as indicated by ASHRAE Thermal Guidelines for IT equipment cooling systems for data centres in the *A1 Category* [58]. The temperature of the air returning from the DC is set according to indications of the technical–scientific literature to ensure IT equipment reliability [20,59]. The temperature ranges of Case A and Case B were selected to assess the trade-off between compressor electricity consumption and the quality of recoverable waste heat, and to evaluate their impact on the overall system performance.

A 500 kW data centre is considered. Based on commonly adopted industry classifications, the 500 kW data centre considered in this study falls within the range of edge data centres, which typically operate between 50 kW and 2 MW. These facilities are designed to provide distributed computing capacity close to end users and are increasingly deployed in urban environments [60].

For the calculation, two fundamental assumptions were made, based on the wide and consolidated literature on the topic:

1. The cooling capacity required for the DC IT equipment equals the installed electrical power, assuming that all electrical load is dissipated as heat [21,29];
2. The electrical consumption of DC IT equipment power is assumed to be constant throughout the year [32,35,36].

For the district-heating network, real, annual hourly profiles of thermal levels and the required thermal power were considered.

As this is a theoretical thermodynamic study on a possible integration between DC and DHN, the distance between DC and the network was not taken into account. Consequently, heat losses in the connection pipelines and the additional pumping power required for fluid transport are not included in the energy and exergy balances. This assumption allows the analysis to focus on the coupling efficiency of the generation and storage technologies and to isolate the thermodynamic and exergetic performance of the proposed DC–HP–TCS-DHN configuration. Typical urban integrations between edge data centres and district-heating networks are characterised by separation distances on the order of tens to a few hundreds of metres; for such distances, transport-related losses and pumping penalties are expected to remain limited compared to the recovered thermal power, and are not expected to alter the qualitative conclusions of the present analysis. Nevertheless, it is acknowledged that in a real-world implementation, the physical distance between systems would represent a constraining factor affecting both overall efficiency and economic feasibility, and would require a site-specific engineering and techno-economic assessment. The present work should, therefore, be interpreted as a best-case thermodynamic assessment of the proposed integration concept.

The thermodynamic simulations were performed using *Python* software.

2.1. Scenario S0. No Integration Between DC and DHN

In Scenario S0, the DC is cooled by its own cooling system, and the DHN is powered by its own thermal plant (Figure 1). There is only one VCC (VCC 1), which cools the data centre and rejects the heat into the outdoor environment: the evaporator cools the working air flow of the data-centre space, and the outdoor air is heated by the condenser of the

cycle. The central generation space of DHN contains the boilers, fuelled by natural gas, which provide the hot water to the network.

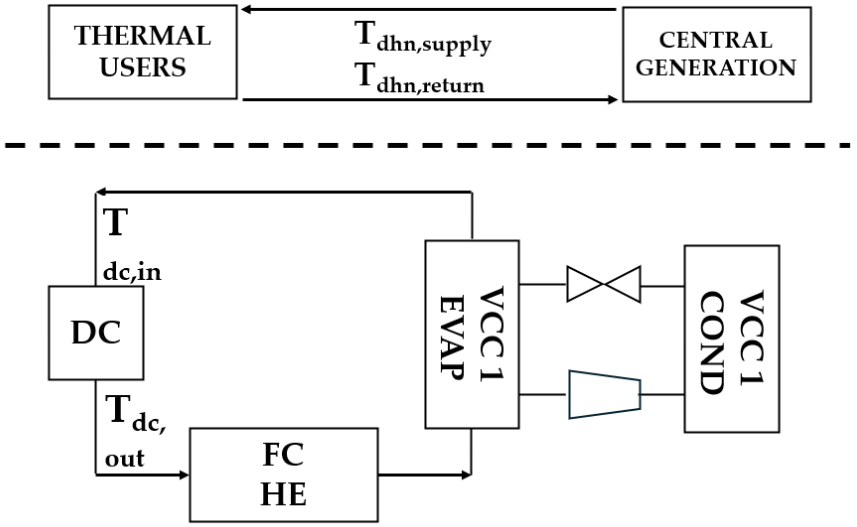


Figure 1. Schematisation of Scenario S0 (no integration between DC and DHN).

2.1.1. DC Non-Integrated Cooling

A hybrid air-based cooling system is considered. It operates in indirect air-side free cooling (FC mode) when the external air temperature is below a fixed threshold ($\mathbf{T}_{\mathbf{lim\ FC}}$), while a vapour-compression cooling system (AC mode) is activated when the external temperature exceeds the limit (no combination of the two modes was considered). The cooling system activates the air-conditioning mode only when the outdoors is hotter than the threshold value and free cooling is not useful.

The cooling power required for the IT equipment ($\mathbf{Q}_{\mathbf{DC,\ cold}}$) equals the generated heat load; the cooling power and the airflow rate of cooling air provided to the DC (m_{DC}) in both modes are related as follows:

$$Q_{DC,\ cold} = c_p \cdot m_{DC} \cdot \left(T_{DC,\ out} - T_{DC,\ in}\right) \quad (1)$$

The external airflow rate required in the FC mode to achieve the desired cooling thermal power is determined by setting the heat exchanger effectiveness ($\mathbf{eff}_{\mathbf{he}}$), defined as the ratio between the effectively exchanged heat and the maximum exchangeable heat. The exchanged heat is set equal to the required cooling capacity (in FC, it is the same as the DC thermal load). The effectiveness is constant and equal to:

$$eff_{he} = \frac{Q}{Q_{max}} \quad (2)$$

The outdoor airflow in the FC mode is modulated in order to achieve the proper supply temperature, also when the outdoor temperatures are low.

Given the known airflows, both on the DC side and the outdoor ambient side, it is possible to calculate the power consumption of the fans ($\mathbf{W}_{\mathbf{f}}$) and the corresponding annual energy consumption, assuming proper pressure drops (**DPs**) across the heat exchanger and fan efficiency ($\mathbf{eff}_{\mathbf{f}}$):

$$W_f = \frac{m \cdot DP}{d \cdot eff_f} \quad (3)$$

When the external temperature is too high to use the FC mode, a VCC (air-to-air) is needed to provide the required cooling power. In AC mode, power consumption includes

the fans and the compressor of the VCC ($\mathbf{W_{comp}}$). To calculate the power consumption of AC, it is necessary to estimate the Energy Efficiency Ratio (**EER**) of the cycle. To do that, a polynomial model for **EER** as a function of saturation levels of the refrigerant was adopted, referring to the data of available commercial models [61] (a validation of the polynomial formulation of **EER** is reported in the Supplementary Materials file of [62]). By setting the pinch-point temperature difference at both the evaporator and condenser ($\mathbf{DT_{PP}}$) and the sink temperature difference ($\mathbf{DT_{sink}}$), the two saturation temperature levels of the refrigerant can be determined. Additionally, a check was conducted to ensure a minimum allowable temperature lift ($\mathbf{DT_{comp,min}}$) between the saturation temperatures of the refrigerant, according to commercially available models of VCC equipment.

Given the relation between the **EER** and ambient temperature, it is possible to calculate the power consumption of the compressor and the heat rejected to the environment ($\mathbf{Q_{sink}}$). The power requirements for the fans of the evaporator and the condenser can be calculated from (2), as done for the FC mode.

$$W_{comp} = \frac{Q_{DC\,,\,cold}}{EER} \quad (4)$$

$$Q_{sink} = Q_{DC,\,cold} + W_{comp} \quad (5)$$

It is also useful to evaluate the efficiency of the VCC of AC mode in terms of the second law of thermodynamics. In this sense, first, the ideal EER ($\mathbf{EER_{id}}$) is evaluated as:

$$EER_{id} = \frac{T_L}{T_H - T_L} \quad (6)$$

where $\mathbf{T_L}$ and $\mathbf{T_H}$ are the low and high saturation temperatures of the refrigerant of the VCC (here expressed in Kelvin). Then, the second-law EER ($\mathbf{EER_{II}}$) is defined as:

$$EER_{II} = \frac{EER}{EER_{id}} \quad (7)$$

It is worth noting that the $\mathbf{EER_{id}}$ was evaluated considering the refrigerant sides (evaporating and condensing temperatures of the VCC refrigerant) and not the source sides, which vary their temperature during the processes.

All the conditions imposed for FC and AC modes are summarised in Table 1.

Table 1. Regulation of FC and AC modes.

FC Operations and Air Loops			**VCC (AC Mode)**		
$T_{DC,in}$	°C	20.0 (A) 25.0 (B)	DT_{pp}	5.0	°C
$T_{DC,out}$	°C	35.0 (A) 40.0 (B)	$DT_{comp,min}$	10.0	°C
$T_{lim\ FC}$	°C	15.0 (A) 20.0 (B)	DT_{sink}	10.0	°C
eff_{he}		0.8	**Thermophysical properties**		
DP heat exch. [63]	Pa	150.0	c_p	kJ/kg/K	1.0
eff_f		0.6	d	kg/m^3	1.2

2.1.2. DHN Non-Integrated Generation System

The hourly annual data for the DHN used in this paper pertain to the Varna network (Bulgaria): the real data were provided by the company that manages the DHN and is a partner of the THUNDER consortium [57]. Table 2 shows the hourly trends and the ranges

(minimum, average, and maximum values) for the network thermal power. The central plant is a boiler which uses natural gas as fuel.

Table 2. Operative ranges of the DHN.

		Minimum	Average	Maximum
Q_{DHN}	MW	3.0	9.3	29.6

As defined in [8,9,11], this DHN can be qualified as a third-generation network. The overall annual energy demand of the DHN in this case study is 81,162 MWh/y. Figure 2 shows the annual thermal request of the DHN. The profile reflects the typical seasonality of the served area: the high demand in winter months covers both space heating and domestic hot water, whereas the lower, flatter profile observed from June to September corresponds almost exclusively to the domestic hot water base-load. The transitional periods in May and October show the gradual switch-off and switch-on of the space heating systems, consistent with the climatic conditions of Varna.

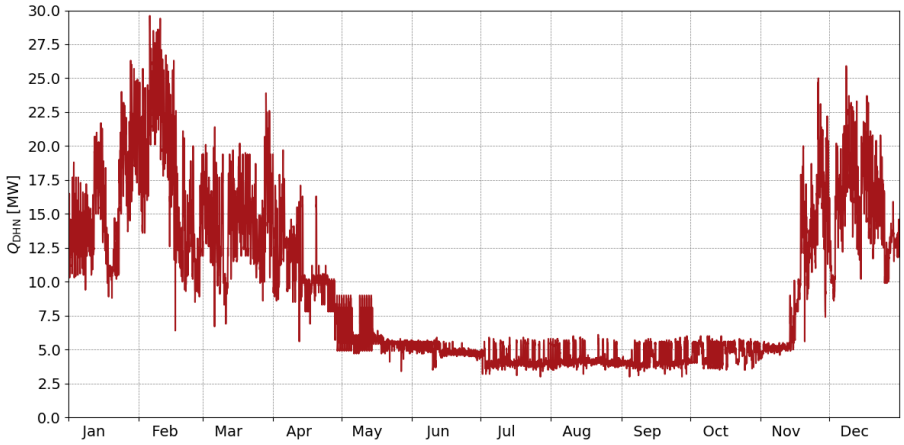


Figure 2. Annual thermal request of DHN.

2.2. Scenario S1. Integration of DC Waste Heat into the DHN

In Scenario S1, the DC cooling system is integrated with the district-heating network through a heat recovery and valorisation process (Figure 3). The utilisation of a thermochemical energy storage (TCS) was assumed, in order to store the wasted and recovered heat from the DC (maximum production in summer with AC mode) and use it when effectively useful (winter requirement from the DHN). The entire process is:

1. A first VCC (VCC 1) cools the data centre and releases heat, which becomes the source for a second VCC (VCC 2);
2. The second VCC (VCC 2) upgrades the heat flow, releasing the heat in the thermal storage during the charging phase;
3. A third VCC (VCC 3) recovers heat from the thermochemical storage during the discharging phase and upgrades it at the proper temperature of DHN.

Steps 1 and 2 happen when AC mode is active (recovery of waste heat from the data centre and charging of thermal storage), mostly in summer. Step 3, the activation of VCC 3, happens when the DHN has a high thermal request, mostly in winter. FC mode is still used when the outdoor temperature is suitable for this scope. In the picture, the connection loops VCC 1–VCC 2, VCC 2–TCS, TCS–VCC 3, and VCC 3–DHN are represented only with the related thermal fluxes. In a real-world application, all these connections could be realised via water loops. Although these loops were not represented in the pictures and modelled in detail, the necessary temperature lifts were properly considered. In Figure 3,

$\mathbf{Q_{waste}}$ is the waste heat from the data centre (VCC 1–VCC 2); $\mathbf{Q_{charg}}$ (VCC 2–TCS) is the heat that charges the thermal storage; $\mathbf{Q_{disch}}$ is the heat discharged from the thermal storage (TCS–VCC 3); $\mathbf{Q_{integ}}$ is the heat integrated in the DHN from the recovery system (VCC 3–DHN).

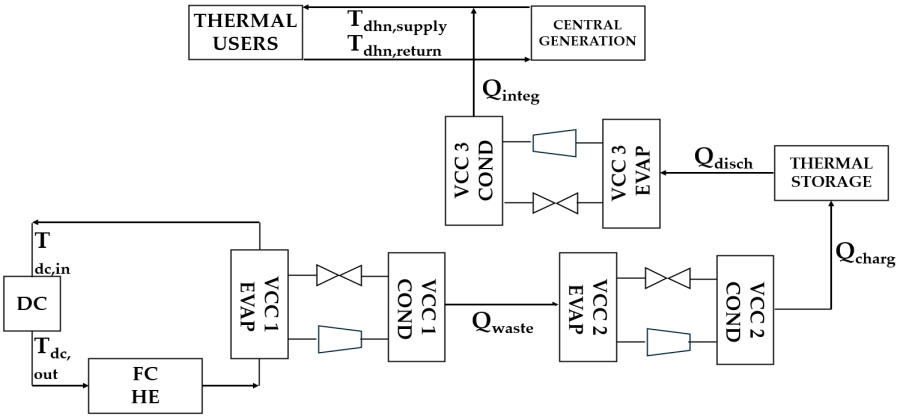


Figure 3. Schematisation of Scenario 1 (integration between DC and DHN).

2.2.1. DC Integrated Cooling, Thermal Recovery, and Upgrade

The thermodynamic modelling of the DC cooling system (VCC 1) is similar to Scenario S0, where heat is rejected to the ambient air; however, in this case, the heat sink is no longer the environment but the second VCC (VCC 2). The discharging of the thermal storage is done with the third VCC (VCC 3).

The modelling of the VCC 2 and VCC 3 is done very similarly to VCC 1, with the difference that the **EER** is evaluated not with a polynomial correlation (due to higher operative temperature not compatible with the approximation range of the polynomial function), but assuming a value of 0.5 for $\mathbf{EER_{II}}$, and so deriving the **EER** from $\mathbf{EER_{II}}$ and $\mathbf{EER_{id}}$ (evaluated with the refrigerant saturation temperatures). This value represents a suitable estimation for large-scale industrial heat pumps, which typically exhibit second-law efficiencies in the range of 0.45–0.55 under realistic operating conditions [64].

2.2.2. TCS Characterisation and Functioning

The thermal storage is charged using the waste heat from the data centre when the AC mode is active, while no recovery was considered during the FC mode. Therefore, the waste heat considered for recovery is the rejection heat produced by the condenser of the VCC 1, which cools the data centre.

The thermochemical storage system was modelled as a black box, where the operational parameters subject to optimisation are the charging and discharging temperatures. The charging temperature is set at 80 °C and the discharge at 40 °C, with a round-trip efficiency of 0.9. These values were derived from experimental tests performed by the Authors as part of the THUNDER project activities. This approach does not consider internal reactions, allowing for a simplified implementation into energy-system models: the focus is placed on its macroscopic behaviour, facilitating the evaluation of system-level performance.

In this context, the role of VCC 2 is not to upgrade heat for immediate use, but to provide the temperature driving force required to store energy in the form of chemical potential, while the VCC 3 connects the TCS and DHN. A sensible low-temperature storage tank operating around 40 °C would mainly enable short-term buffering and would become impractical for seasonal decoupling due to the large volume required and

standing thermal losses. Therefore, the 80 °C charging level was adopted to enable seasonal storage through TCS.

2.3. Exergy Analysis

The exergy efficiency is a key metric for assessing the thermodynamic performance of energy-recovery systems. In the context of waste heat recovered from data centres, stored in a thermochemical storage system and subsequently delivered to a district-heating network, exergy analysis enables the evaluation of energy quality and the identification of irreversibility throughout the process. This approach supports the design of sustainable and high-efficiency energy solutions by highlighting opportunities for system optimisation. In exergy analysis, a distinction is made between exergy destruction and exergy losses. Exergy destruction refers to the internal irreversibility within a system, such as friction, heat transfer across finite temperature differences, or chemical reactions, which degrade the quality of energy and are governed by the second law of thermodynamics. Exergy losses, on the other hand, represent the exergy that leaves the system boundaries without being utilised, typically discharged to the environment. While both contribute to the overall inefficiency, only destruction is associated with intrinsic thermodynamic irreversibility. The dead state for all calculations is defined at $T_0 = 273.15\,K$ and $P_0 = 101.325\,kPa$.

The exergy balances for each component are summarised below.

2.3.1. Data-Centre Cooling

The cooling of the IT infrastructure is modelled through both passive and active stages. The exergy destruction during the free-cooling mode is defined as:

$$EX_{D,FC} = \dot{m}_{DC} \cdot (ex_{out,\ DC} - ex_{in,\ DC}) \quad (8)$$

where the irreversibility is strictly linked to the air-temperature lift required to maintain the server environment. When ambient conditions necessitate active cooling, the VCC components are evaluated. For the evaporator and condenser, the exergy destruction reflects the heat transfer across finite temperature differences; the compressor represents the primary form of irreversibility of the system.

$$EX_{D,evap} = \dot{m}_{ref} \cdot (ex_{ref,\ in} - ex_{ref,\ out}) + \dot{m}_{DC} \cdot (ex_{air,\ in,evap} - ex_{air,\ out,evap}) \quad (9)$$

$$EX_{D,evap} = \dot{m}_{ref} \cdot (ex_{ref,\ in} - ex_{ref,\ out}) + \dot{m}_{water} \cdot (ex_{water,\ in,\ cond} - ex_{water,\ out,\ cond}) \quad (10)$$

$$EX_{D,cond} = \dot{m}_{ref} \cdot (ex_{ref,\ in} - ex_{ref,\ out}) + \dot{m}_{air,ext} \cdot (ex_{air,\ in,\ cond} - ex_{air,\ out,\ cond}) \quad (11)$$

$$EX_{D,cond} = \dot{m}_{ref} \cdot (ex_{ref,\ in} - ex_{ref,\ out}) + \dot{m}_{water} \cdot (ex_{water,\ in,eva} - ex_{water,\ out,eva}) \quad (12)$$

$$EX_{D,comp} = W_{comp} + \dot{m}_{ref} \cdot (ex_{refr,\ in} - ex_{refr,\ out}) \quad (13)$$

$$EX_{D,valve} = \dot{m}_{ref} \cdot (ex_{ref,\ in} - ex_{ref,\ out}) \quad (14)$$

Equation (9) is used for the evaporator of VCC 1 (evaporation on the DC side) in both scenarios; Equation (10) for the evaporators of VCCs 2 and 3 (evaporation on VCC 1 and TCS, respectively, via water loops) in the integrated scenario; Equation (11) for the condenser of VCC 1 in the non-integrated scenario (condensation on the outdoor air); Equation (12) for the condensers of VCC 2 and VCC 3 (condensation on the TCS and DHN, respectively, via water loops) in the integrated scenario; Equation (13) for the compressor of all VCCs; and Equation (14) for the throttling valve of all VCCs.

2.3.2. Thermochemical Storage

The exergy balance for the TCS unit accounts for the losses during the adsorption/desorption cycles:

$$EX_{D,TCS} = \dot{m}_{water,\,charg} \cdot (ex_{in} - ex_{out}) - \dot{m}_{water,\,disch} \cdot (ex_{in} - ex_{out}) \quad (15)$$

This formulation was chosen to capture the degradation of the thermal potential during the chemical reaction and the storage period, providing a clearer picture of the round-trip efficiency.

2.3.3. District-Heating Network

The integration logic involves supplementing the traditional gas boiler. The exergy destruction of the boiler is calculated as:

$$EX_{D,boiler} = \dot{m}_{gas} \cdot (ex_{gas,\,in} - ex_{gas,\,out}) + Q_{in,\,boiler} \cdot \left(1 - \frac{T_0}{T_{source}}\right) \quad (16)$$

The inclusion of the Carnot factor is essential here; it quantifies the high-grade chemical exergy of the fuel that is "degraded" into lower-temperature thermal energy. Furthermore, the heat exchanger (HE) performance is split into internal destruction ($\mathbf{EX_{D,HE}}$), caused by the temperature gradient between flue gas and water, and external loss ($\mathbf{EX_{L,HE}}$), representing the exergy discarded to the environment via exhaust gases:

$$EX_{D,HE} = \dot{m}_{DHN} \cdot (ex_{DHN,\,in} - ex_{DHN,\,out}) + \dot{m}_{gas} \cdot (ex_{gas,\,in} - ex_{gas,\,out}) \quad (17)$$

$$EX_{L,HE} = \dot{m}_{gas} \cdot (ex_{gas,\,out} - ex_{gas,\,in}) \quad (18)$$

The heat exchanger transfers heat between combustion gases and water. Losses are due to inefficiencies in thermal exchange.

2.3.4. Exergy Efficiency

The system efficiency for Scenario S0 is:

$$\eta_{ex} = \frac{\dot{m}_{DHN} \cdot (ex_{out} - ex_{in})}{W_{comp,VCC1} + \dot{m}_{DC} \cdot (ex_{DC,\,out,} - ex_{DC,in}) + Q_{boiler,in} \cdot \left(1 - \frac{T_0}{T_{source}}\right)} \quad (19)$$

The system efficiency for Scenario S1 is:

$$\eta_{ex} = \frac{\dot{m}_{integ} \cdot (ex_{out,water,integ} - ex_{in,water,integ}) + \dot{m}_{DHN} \cdot (ex_{out} - ex_{in})}{W_{comp,VCC1} + W_{comp,VCC2} + W_{comp,VCC3} + \dot{m}_{DC} \cdot (ex_{DC,\,out,} - ex_{DC,in}) + Q_{boiler,in} \cdot \left(1 - \frac{T_0}{T_{source}}\right)} \quad (20)$$

where $\dot{\mathbf{m}}_{\mathbf{integ}}$ represents the fraction of the district-heating flow diverted from the main stream, serving as the heat sink for the heat pump that recovers thermal energy from the thermochemical storage.

2.3.5. General Overview of Exergy Analysis Contributions for Scenario S0

In the non-integrated scenario, exergy destruction and exergy losses are calculated independently for the DC and DHN. The thermodynamic inefficiencies associated with each subsystem are assessed separately, without accounting for potential synergies or interactions. As a result, the overall system performance may be underestimated, and opportunities for integrated optimisation might be overlooked. Table 3 outlines, for each component, whether it accounts for destructions or losses. For the data centre, the components contributing to exergy destruction and losses include the evaporator, compressor, condenser, expansion valve, and the heat exchanger used for free cooling. In the DHN, the main sources of inefficiencies are the boiler and the heat exchanger.

Table 3. Exergy destructions and losses, Scenario S0.

Exergy Destructions	Exergy Losses
VCC 1 Evaporator	VCC 1 Condenser
VCC 1 Compressor	DHN Heat Exchanger
VCC 1 Condenser	DC Free Cooling
VCC 1 Valve	
DHN Boiler	
DHN Heat Exchanger	
DC Free Cooling	

2.3.6. General Overview of Exergy Analysis Contributions for Scenario S1

In the integrated scenario, DC and DHN are considered as a single thermodynamic system, allowing for a comprehensive evaluation. This approach enables the identification of synergies between subsystems and a more accurate quantification of overall exergy destruction and losses: it becomes possible to highlight the benefits of integration in terms of improved energy quality utilisation and reduced irreversibility. Table 4 outlines, for each component, whether it accounts for destructions or losses.

Table 4. Exergy destructions and losses, Scenario S1.

Exergy Destructions	Exergy Losses
VCC 1 Evaporator	DHN Heat Exchanger
VCC 1 Compressor	DC Free Cooling
VCC 1 Condenser	
VCC 1 Valve	
VCC 2 Evaporator	
VCC 2 Compressor	
VCC 2 Condenser	
VCC 2 Valve	
VCC 3 Evaporator	
VCC 3 Compressor	
VCC 3 Condenser	
VCC 3 Valve	
DHN Boiler	
DHN Heat Exchanger	
DC Free Cooling	
TCS	

3. Results and Discussion

In this section, the results of the energy and exergy analysis of the different scenarios are reported and compared in terms of the performance of data-centre cooling systems and waste-heat recovery and reutilisation.

3.1. Energy Analysis Results

This paragraph is dedicated to the energy analysis of the two scenarios.

3.1.1. Scenario S0. Non-Integrated System

The combination of indirect free cooling and VCC active cooling in the data centre results in an electricity consumption and waste heat, as reported in Table 5.

Table 5. Annual electricity consumption and waste-heat production of data-centre cooling system, Scenario S0.

Case	Electricity FC	Electricity AC	Electricity Tot	Waste Heat FC	Waste Heat AC	Waste Heat Tot
	MWh	MWh	MWh	MWh	MWh	MWh
A	23.6	217.3	240.9	2611.5	1985.1	4596.6
B	29.2	103.0	132.2	3439.5	1043.1	4482.6

Switching from Case A to Case B, there is a consistent reduction in the electricity consumption of the data-centre cooling system (almost 45.0%) due to the larger use of free cooling. Regarding the waste-heat production, it is necessary to underline that, when the FC mode is operating, the waste thermal flux is made by the outdoor airflow heated at the free-cooling heat exchanger, so at a temperature lower than the exhaust temperature of the data centre (35.0 °C for Case A, 40.0 °C for Case B). Due to these relatively low temperatures, it has been chosen—as the control logic of waste-heat recovery and energy-storage charging—to use only the waste heat deriving from the production of the VCC condenser during the AC mode operations. In Case B, the effectively recoverable waste heat is almost 45.0% with respect to Case A, raising necessary questions concerning the regulation of the cooling system of the data centre in relation to the heat recovery purpose.

The annual trends of electricity consumption and waste-heat production are reported in Figures 4 and 5.

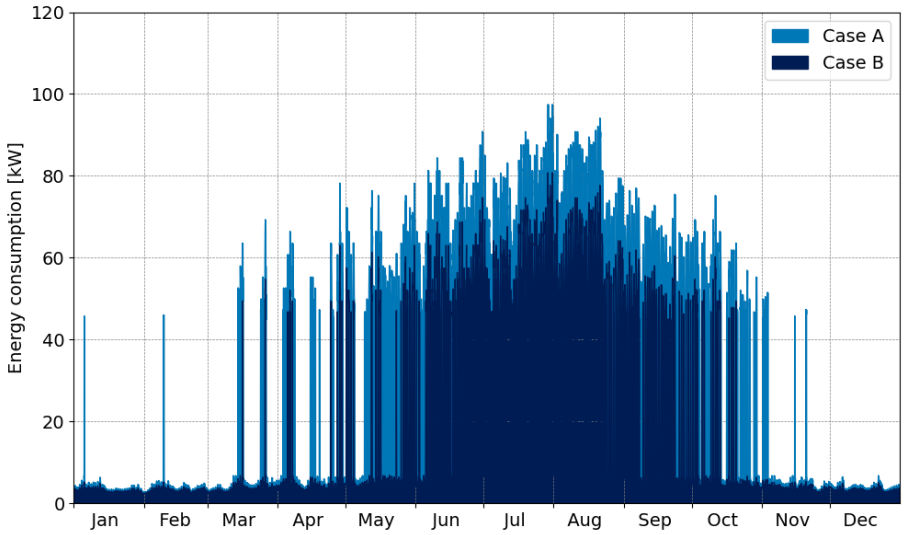


Figure 4. Electricity consumption of DC cooling system, Scenario S0.

The profile of the electricity consumption observed in Figure 4 is strictly linked to the thermodynamics of the VCC. During the summer months, the high outdoor air temperature imposes a higher condensing temperature on the refrigeration cycle. This increases the pressure ratio across the compressor, leading to higher work input ($\mathbf{W_{comp}}$) for the same cooling duty request, and consequently a lower **EER**. Conversely, in the transition months, the lower ambient temperature allows for lower condensing temperatures and better EER. The peaks in consumption correspond to the hottest hours of the year, where the system operates at its lowest thermodynamic efficiency.

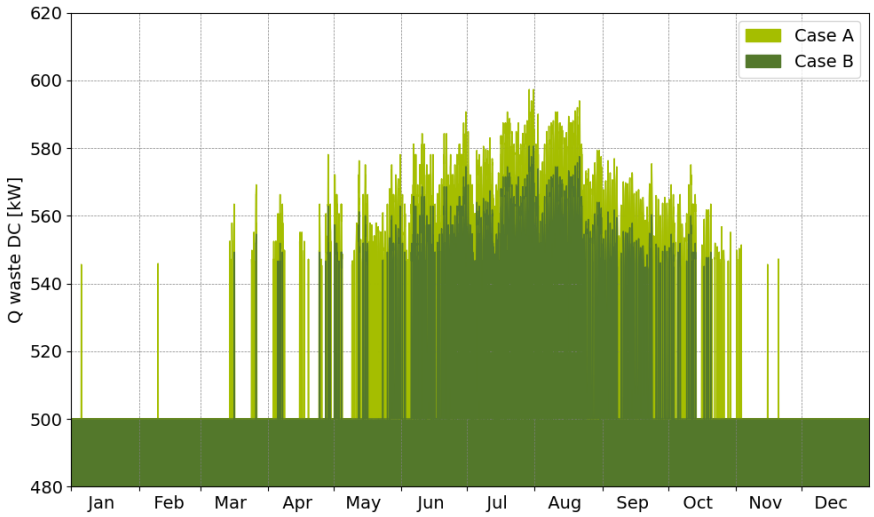


Figure 5. Heat discharged from DC cooling system, Scenario S0.

This behaviour is clearly depicted in Figure 6 (Case A) and Figure 7 (Case B), which compare the hourly EER of the baseline system with the integrated one.

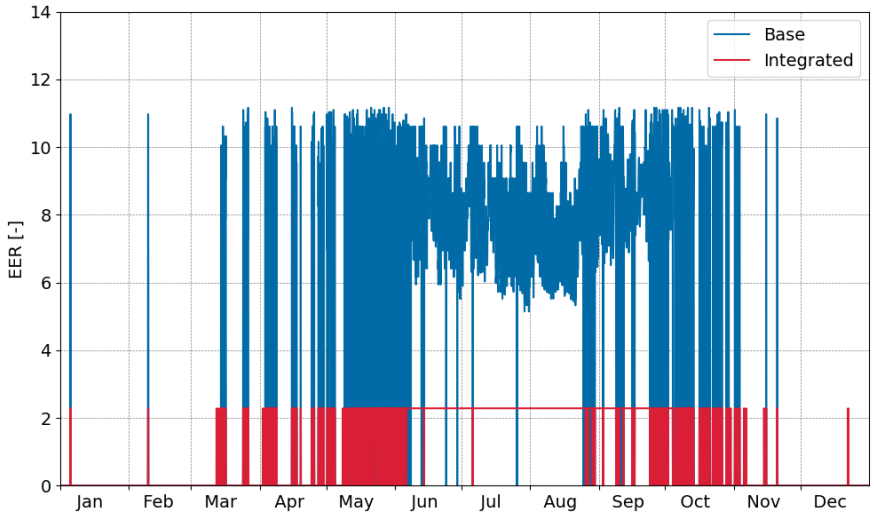


Figure 6. Hourly comparison of the Energy Efficiency Ratio (EER) for Case A.

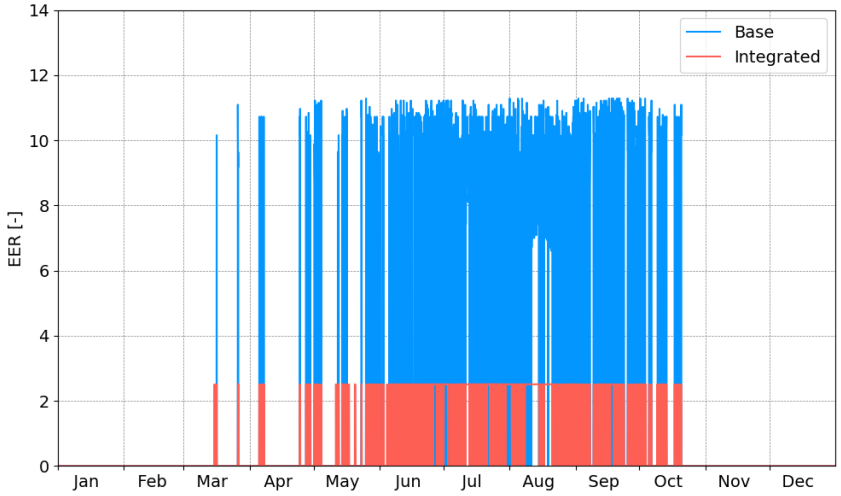


Figure 7. Hourly comparison of the Energy Efficiency Ratio (EER) for Case B.

Scenario S0 (blue trend) exhibits strong fluctuations driven by ambient conditions, with efficiency drops during summer peaks. In stark contrast, Scenario S1 (red trend) shows a constant EER profile during active cooling operation. This is because the combined system (VCC 1 + VCC 2) operates between controlled temperature levels, evaporating at the DC temperature and condensing at the fixed TCS charging temperature (80 °C), thus decoupling the process efficiency from outdoor weather conditions. It is worth noting that the lower absolute value of the combined EER in the integrated scenario (approximately 2.3) compared to the baseline is the thermodynamic cost of the higher temperature lift required to upgrade the waste heat for storage purposes.

Regarding the district-heating network, the annual consumption of thermal energy is 97,522 MWh/y, corresponding to 9122 Sm^3 of natural gas (considering that 1 Sm^3 is equivalent to 10.7 kWh).

3.1.2. Scenario 1. Integration of DC Waste Heat into the DHN Through TCM

Scenario S1 includes the integration of waste heat from DC into the DHN through a thermochemical energy storage system. Waste heat is produced at the condenser of VCC 1, and upgraded at the necessary thermal level of thermochemical storage via the VCC 2. VCC 3 discharges the storage, releasing heat into the district-heating network.

The combination of indirect free cooling and VCC 1 active cooling in the data centre results in an electricity consumption and waste heat, as reported in Table 6.

Table 6. Annual electricity consumption and waste-heat production of data-centre cooling system, Scenario S1.

Case	Electricity FC	Electricity AC	Electricity Tot	Waste Heat FC	Waste Heat AC	Waste Heat Tot
	MWh	MWh	MWh	MWh	MWh	MWh
A	22.7	805.1	827.8	2 542.0	2 159.3	4 701.3
B	27.8	414.0	441.8	3 342.5	1 185.8	4 528.3

In the table, "Waste Heat AC" refers to the heat produced at the condenser of VCC 1 during AC operations, and represents the thermal source of VCC 2.

Switching from Case A to Case B, there is a consistent reduction in the electricity consumption of the data-centre cooling system (almost 45.0%, with the same logic as Scenario S0), but this fact implies an equal reduction in the availability of waste heat during the AC mode due to the larger use of free cooling and better EER.

This point is crucial in the coupling sector of data-centre cooling and district-heating networks. The increase in electrical consumption on the part of the data-centre operator—derived from higher operative temperatures in the supply air to the IT equipment—must clearly be offset by benefits, including economic ones, arising from the savings that the district-heating operator can achieve in terms of reduced thermal energy supplied to the network. This trade-off highlights that the "optimal" operating condition for the IT equipment is not a fixed parameter when looking at the integrated system. While Case A and Case B explore two static boundaries (prioritising heat recovery vs. prioritising DC electrical efficiency), a fully optimised control strategy would likely operate dynamically between these limits. For instance, during periods of peak DHN demand, the system could favour the Case-A approach to maximise heat recovery, whereas, in periods of low thermal demand, it could shift towards Case B to minimise electricity consumption via free cooling.

Comparing the same cases with respect to Scenario S0, in Scenario S1, there is an increase in both electricity consumption and waste-heat production—considering VCC 1 and VCC 2 together as a single system in Scenario S1—of almost 2.5 times.

The "chain" of thermal integration (waste heat VCC 1 → VCC 2, charging heat VCC 2 → TCS, discharging heat TCS → VCC 3, integration heat VCC 3 → DHN) is reported in Table 7.

Table 7. Waste heat recovery and reutilisation process, scenario S1.

Case	Waste Heat VCC 1 → VCC 2	Charging Heat VCC 2 → TCS	Discharging Heat TCS → VCC 3	Integration Heat VCC 3 → DHN
	MWh	MWh	MWh	MWh
A	2159.3	2643.1	2378.8	2469.8
B	1185.8	1541.5	1306.4	1356.4

The energy stored in the TCM coming from the DC waste-heat recovery process is 2643.1 MWh in Case A and 1541.5 MWh in Case B (final value of the recovery from DC, steps VCC 1 → VCC 2 and VCC 2 → TCS). The greater value of waste heat for Case A is related to the lower evaporation temperature, so lower EER, of the VCC 1 (as in Scenario S0). The greater values of both cases with respect to Scenario S0 derive from the higher values of the final condensation temperature (condensation temperature of VCC 2, required to charge the TCS). Considering an efficiency of the TCS (heat released/heat charged) equal to 0.9, it leads to 2378.8 and 1306.4 MWh, respectively, being released into the DHN. In a real-world application, this efficiency obviously depends on the operative conditions, but it is in accordance with the experimental values obtained by the Authors during experimental activities.

Considering the small size of DC compared to that of district heating, this energy accounted for 3.0% (Case A) and 1.7% (Case B) of the total demand of the DHN. The maximum percentage of waste heat in the DHN is almost 22.4% (Case A) and 21.8% (Case B); the annual trend is shown in Figure 8.

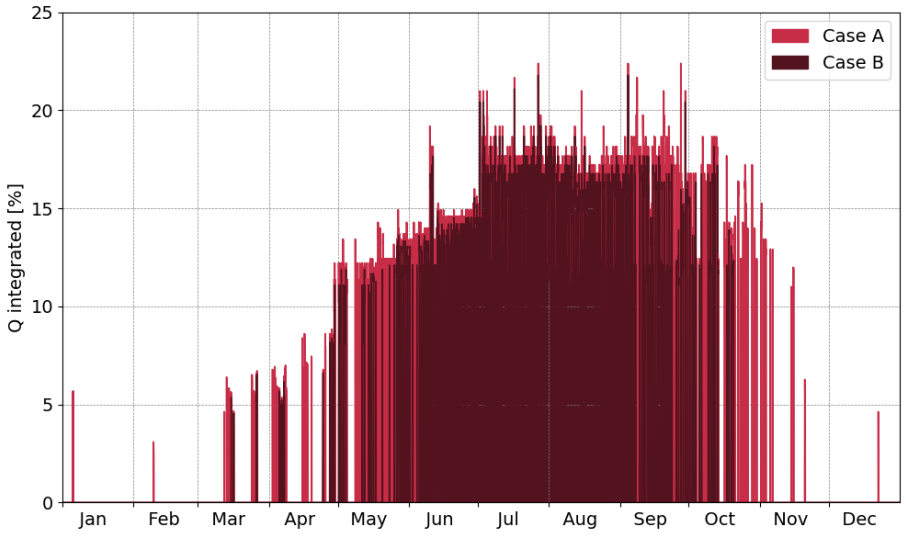


Figure 8. Heat integrated in DHN, Scenario S1.

The absolute value of data-centre waste heat integrated into the district-heating network seems to be small (due to the small size of the data centre), but it is not negligible. The vital point is not only the possibility to effectively use the waste heat in the DHN, but the possibility to avoid the release of thermal energy into the environment surrounding the data centre (regardless of its size), with a significant impact in terms of reducing the urban heat island effect.

3.1.3. Comparison of VCC System Consumption Between Scenario 0 and Scenario 1

The instantaneous electricity consumption of the base non-integrated solution—Scenario S0 (VCC 1)—and the integrated solution—Scenario S1 (VCC 1 + VCC 2)—is reported in Figure 9, at the top for Case A and at the bottom for Case B. In the base scenario, the electricity consumption varies according to the variation in outdoor air temperature: the cooling system, in AC mode, is condensed by the outdoor air; consequently, the EER depends on it. In the integrated scenario, the electricity consumption of VCC 1 + VCC 2 is constant: VCC 1 always evaporates at the data-centre evaporation condition, VCC 1 condenses, VCC 2 evaporates on the integration (water) loop at a fixed temperature, and VCC 2 condenses at the charging temperature of the TCS, so the EER is constant.

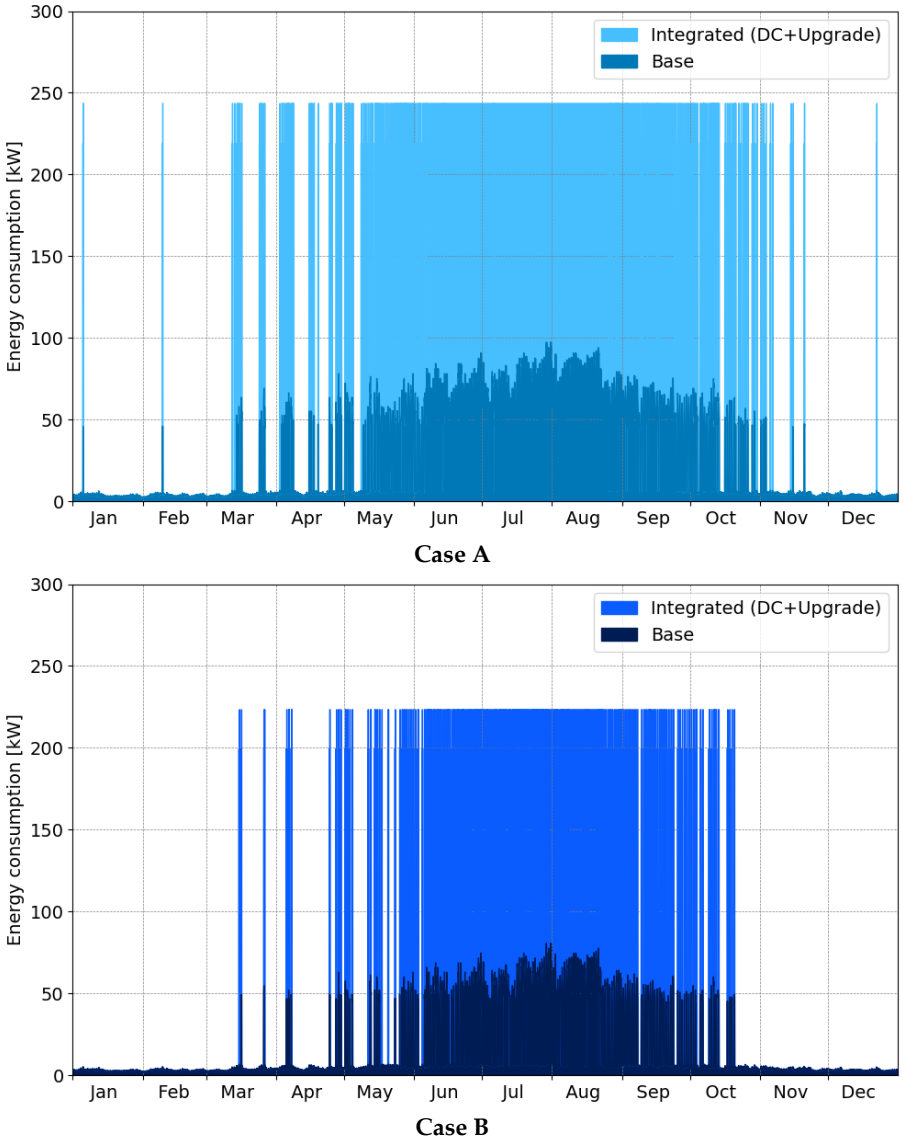


Figure 9. Electricity consumption of the data-centre cooling system.

The difference between the two scenarios is driven by the heat-sink conditions. In the baseline, Scenario S0, the heat sink is the ambient air, which fluctuates significantly, causing the compressor power to vary continuously to maintain the temperature lift. In the integrated Scenario S1, the sink for the first stage (VCC 1) is the evaporator of the second stage (VCC 2), and the sink for VCC 2 is the thermochemical storage charging loop. Since the TCS charging temperature is fixed (e.g., 80 °C) and the internal loops operate at controlled temperatures, the pressure ratios across the compressors remain constant. This

results in the flat electricity consumption profile observed for S1, decoupling the system efficiency from external weather conditions during active cooling operation.

3.2. Exergy Analysis Results

The trends of annual exergy efficiency (η_{II}) and the efficiency difference ($\Delta\eta_{II}$) for the two scenarios are reported as follows:

- Comparison between Scenario S0 and Scenario S1, Case A, Figure 10;
- Comparison between Scenario S0 and Scenario S1, Case B, Figure 11;
- Difference in exergy efficiency between the two scenarios, Case A, Figure 12;
- Difference in exergy efficiency between the two scenarios, Case B, Figure 13.

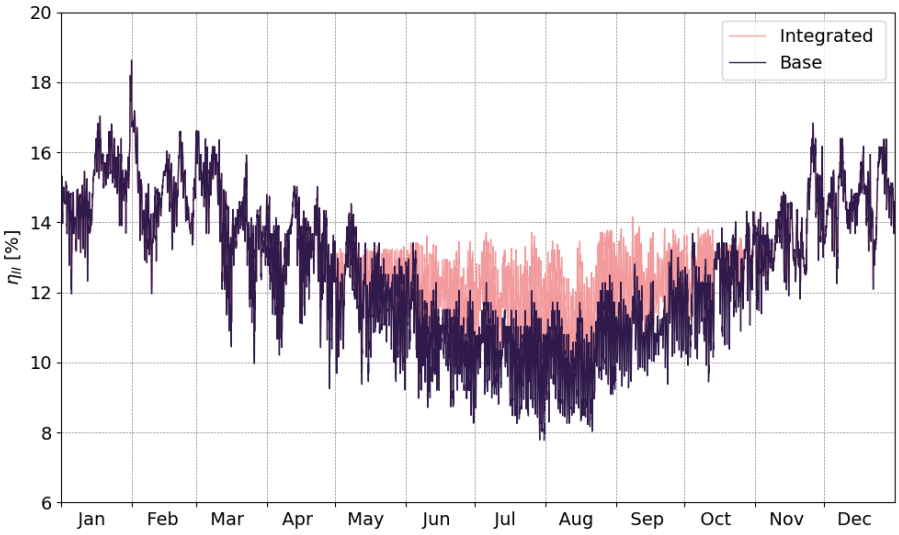


Figure 10. Exergy efficiency for Scenario S0 and Scenario S1, Case A.

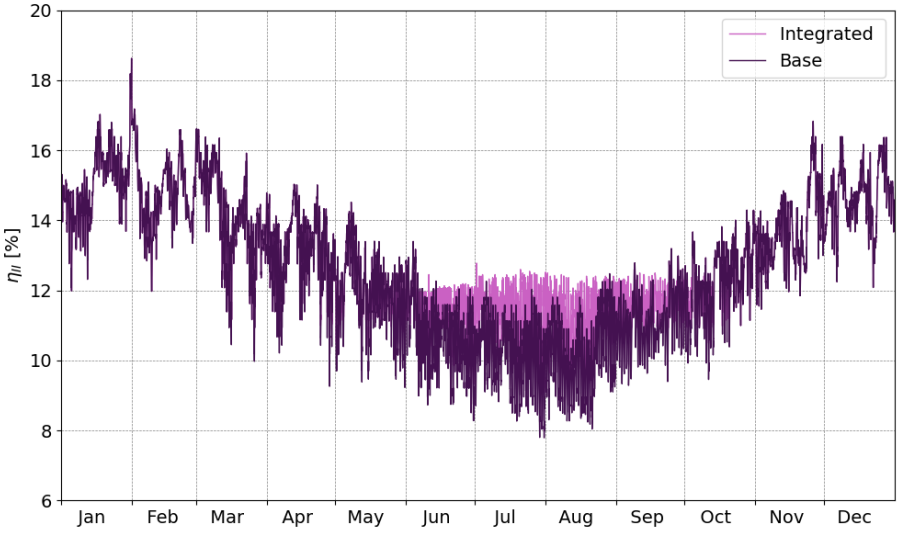


Figure 11. Exergy efficiency for Scenario S0 and Scenario S1, Case B.

The thermodynamic reason for the efficiency drops observed between May and September lies in the increased exergy destruction within the compressors. As the outdoor temperature rises, the temperature difference between the source (DC IT room) and the sink (outdoor air) increases. To overcome this gradient, the compressors must supply more work (high-quality energy). Since the cooling effect represents a thermal exergy transfer at low temperature (low-quality), the ratio of useful exergy output to work input

inevitably decreases. In contrast, during free-cooling operations (winter/intermediate months), the only exergy input is the electrical work for the fans, which is orders of magnitude lower than the compressor work, resulting in significantly higher overall exergy efficiency.

Generally speaking, the higher values of exergy efficiency, for both scenarios and both cases (Figures 10 and 11), are obtained during FC operations (12.0–16.0%). The utilisation of the AC mode during summer months, with the consumption of electricity for the compressors, leads to a reduction in the exergy efficiency (8.0–12.0%).

It is interesting to note that, for the integrated scenario, the best values of exergy efficiency are obtained for Case A because there is a larger "output product" (the waste heat) that could be used inside the integrated systems.

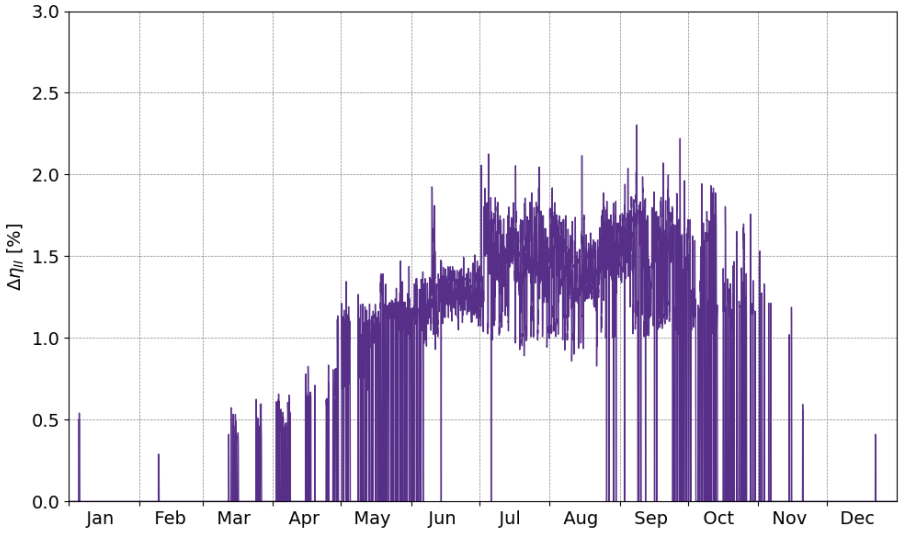


Figure 12. Difference in exergy efficiency for Scenario S0 and Scenario S1, Case A.

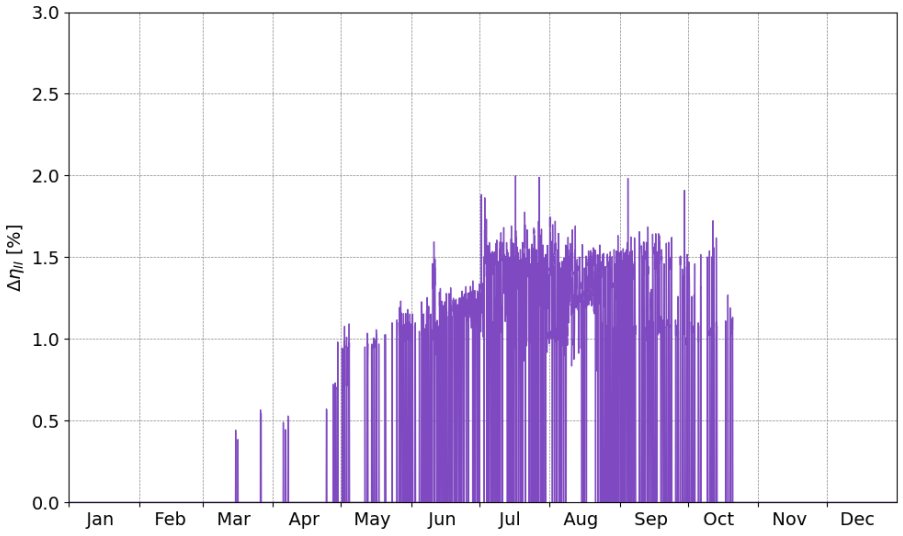


Figure 13. Difference in exergy efficiency for Scenario S0 and Scenario S1, Case B.

From the graphs of exergy efficiency difference, evaluated by the difference between Scenario S1 and Scenario S0 (Figures 12 and 13), it is possible to observe the increase in efficiency with the integrated scenario. Reusing and redirecting the waste heat into the district heating—that is, an "energy waste" towards the outdoor environment in the non-integrated scenario—with the help of TCS, coupling availability, and demand represents a proper way to efficiently use the data centre as a thermal source. The favourable trend

of the integration scenario, in terms of exergetic efficiency, emerges despite the electrical energy required for the operation of VCC 2 and VCC 3 installed for thermal upgrading. The exergy analysis confirms that, in terms of efficient utilisation of energy forms (thermal and electric), the adopted strategy of coupling the DC and DHN via TCS and VCCs is correct.

3.3. Further Possible Strategies for Waste-Heat Use

From the results reported in Table 6, it is possible to observe that there is the availability of a large quantity of waste heat produced during free-cooling operations (2542.0 and 3342.5 MWh/y for Cases A and B, respectively). The production of this thermal flux generally happens in the cold months, when there is also a huge demand from the district-heating network. For a complete integration of data-centre waste heat into a district-heating network, a direct integration of waste heat via a heat pump could be advantageous, particularly if the data centre is located close to the DHN production plant. Given the presence of VCC 2 and VCC 3, it is also possible to recover waste heat during FC operation and integrate it into the DHN after thermal upgrading. In this way, the share of fuel required to meet the DHN demand can be further reduced, thereby further promoting its decarbonisation.

3.4. Further Analysis of the Thermochemical Storage

The results presented in the previous sections are based on assumptions derived from the preliminary experimental activities of the THUNDER project—specifically, a charging temperature of 80 °C and a round-trip efficiency of 0.9. However, given the innovative nature of the technology, it is fundamental to discuss how deviations from these design parameters affect the global performance. The simplified sensitivity analysis shown hereafter focuses on Case A. The relative variations observed for Case A are considered representative for Case B as well, since the thermodynamic behaviour of the upgrading cycle (VCC 2) depends primarily on the temperature lift, which shifts rigidly when changing the DC source temperature.

3.4.1. Effect of Charging Temperature

The charging temperature of the TCS determines the condensation level of the second-stage heat pump (VCC 2). Increasing this temperature (e.g., from 80 °C to 90 °C) to match specific reaction kinetics would require a higher temperature lift from the VCC 2. Thermodynamically, this leads to a reduction in the COP of the upgrading cycle. Sensitivity calculations indicate that a 10 °C increase in charging temperature results in an increase in electricity consumption for the VCC 2 of 25%, causing a consequent drop in the global exergy efficiency of the integrated scenario. Conversely, if the TCS material allows for lower activation temperatures (e.g., 70 °C), the electrical penalty decreases by 19%, making the integration even more competitive.

3.4.2. Effect of Round-Trip Efficiency

The round-trip efficiency accounts for heat losses during the storage period and inefficiencies in the reactor. This parameter has a linear impact on the energy integrated into the DHN. Reducing the TCS efficiency from the assumed 0.9 to a more conservative 0.75 would directly reduce the useful heat output ($\mathbf{Q_{integ}}$) by roughly 17%. From an exergy perspective, a lower TCS efficiency implies that a larger fraction of the high-quality exergy input (electricity used in VCC 2) is dissipated without generating a useful heating effect, thus reducing the global exergy efficiency ($\boldsymbol{\eta_{II}}$).

3.5. Relevance of This Proposal for Low-Temperature District-Heating Networks

Although fourth- and fifth-generation district-heating systems are mentioned in the *Introduction* as part of the broader transition towards low-temperature and more flexible heating networks, the present study deliberately focuses on a real, third-generation DHN currently in operation in Varna (Bulgaria). The objective is not to optimise future network designs, but to assess the feasibility and thermodynamic performance of data-centre waste-heat integration within existing infrastructure. From a conceptual perspective, operating at lower network temperatures, as foreseen in 4GDH/5GDHC systems, would be expected to further improve heat-pump performance, exergy efficiency, and the usable share of low-grade waste heat. However, a quantitative assessment of such effects would require a different network configuration and is, therefore, beyond the scope of the present work. The results presented here should, thus, be interpreted as representative of current-generation district-heating systems, while also providing an upper-level indication of the potential benefits that could be achieved in lower-temperature modern DHNs.

4. Conclusions

In this paper, the possible utilisation of data-centre (DC) waste heat in a real, third-generation district-heating network (DHN), located in Varna (Bulgaria), has been evaluated. The waste heat originates from the data-centre cooling system, which dissipates the thermal load of the IT equipment. Two situations have been compared: a reference configuration with an independently operated data-centre cooling system and district-heating generation plant (*Scenario S0*), and an integrated configuration in which data-centre waste heat is recovered through heat pumps (HPs) and thermochemical energy storage (TCS) and supplied to the district-heating network (*Scenario S1*). Two alternative thermal management strategies for the data centre have been considered in both scenarios (different supply and return temperatures, free-cooling activation). An energy and exergy analysis has been conducted and extended to a full year of operation, on an hourly basis.

For this specific case study, the main results can be summarised as follows:

1. Despite the limited size of the analysed data centre (500 kW), recovered waste heat can supply 3.0% of the annual DHN demand and 22.4% of the instantaneous thermal load during favourable operating periods (Case A);
2. Higher operating temperatures and increased use of free cooling reduce the electricity consumption of the DC but limit the availability of recoverable waste heat, highlighting the need for coordinated strategies between DC and DHN operators.

Beyond the specific case study, several findings have broader relevance for the integration of data-centre waste heat into district-heating systems:

3. The integrated DC–HP–TES–DHN configuration systematically increases the overall exergy efficiency compared to the non-integrated scenario, confirming the thermodynamic advantage of valorising waste heat;
4. Thermochemical storage effectively decouples the temporal mismatch between waste-heat availability and district-heating demand, enabling seasonal heat shifting and increasing the share of usable recovered energy.

While the analysed data centre represents a relatively small, edge-scale facility, the observed trends regarding exergy performance, the role of thermal storage, and the trade-off between data-centre efficiency and heat recovery are expected to remain valid for larger installations and different district-heating network configurations. Overall, the results support the inclusion of data centres among viable urban waste-heat sources and underline the importance of heat-pump- and storage-supported integration schemes to enhance flexibility and accelerate the decarbonisation of existing district-heating networks.

https://doi.org/10.3390/en19030800

Supplementary Materials: The following supporting information can be downloaded at: https://www.mdpi.com/article/10.3390/en19030800/s1.

Author Contributions: Conceptualization, A.R. and L.S.; Methodology, A.V. and L.S.; Software, A.V. and L.S.; Validation, A.V. and L.S.; Formal analysis, L.S.; Investigation, A.V. and L.S.; Resources, L.T., A.R. and L.S.; Data curation, A.V. and L.S.; Writing—original draft, L.S.; Writing—review & editing, L.T. and L.S.; Visualization, A.V. and L.S.; Supervision, L.T., A.R. and L.S.; Project administration, L.T. and A.R.; Funding acquisition, L.T. and A.R. All authors have read and agreed to the published version of the manuscript.

Funding: This research was funded by: the European Union through the project **THUNDER**—*THermochemical storage Utilization eNabling Data centre seasonal Energy Recovery* (Horizon Europe Programme—Call CL5-2023-D3-01—Grant Agreement No. 101136186); the Cassa di Risparmio Project **ATENA**—*Accumuli TErmici iNnovativi tramite materiali Adsorbenti* (Bando Ricercatori 2023—ATENACRF2023.1402—B13C23004220007), in English, *Innovative thermal energy storage through the utilisation of adsorbent materials*. The APC was kindly offered by Dr. Martina Capone and Prof. Elisa Guelpa (Politecnico di Torino).

Data Availability Statement: Data can be made available upon request to the Corresponding Author. The effective sharing of data will be evaluated by all of the Authors.

Conflicts of Interest: The Authors declare no conflicts of interest.

Nomenclature

General abbreviations		
AC	Active cooling mode	
COMP	Compressor of VCC	
COND	Condenser of VCC	
DC	Data centre	
DHN	District-heating network	
EVAP	Evaporator of VCC	
FC	Free-cooling mode	
HE	Heat exchanger	
IT	Information and technology	
VCC	Vapour Compression Cycle	
Thermodynamics		
COP	Coefficient of performance	
c_P	Specific heat at constant pressure of air	kJ/kg/K
d	Density of air	kg/m^3
DP	Pressure drop	Pa
DT	Temperature difference	°C
E	Total exergy	kJ
e	Specific exergy	kJ/kg
EER	Energy Efficiency Ratio	
eff	Efficiency	
m	Mass flow	kg/s
Q	Thermal power	kW
T	Temperature	°C
TCM	Thermochemical material	
TCS	Thermochemical energy storage	
W	Work	kW
Subscripts		
charg	Charging heat of TCS	
cold	Cold effect of VCC	

D	Exergy destruction
disch	Discharging heat of TCS
f	Fan
H	High temperature of VCC
he	Heat exchanger
hot	Referred to hot effect of VCC
id	Ideal
II	Second law of thermodynamics
in	Inlet
integ	Integration heat from the TCS to the DHN
L	Low temperature of VCL (from the context)
L	Exergy loss (from the context)
lim FC	Outdoor air maximum temperature for FC activation
max	Maximum
min	Minimum
out	Outlet
pp	Pinch point
ref	Refrigerant of the VCC
return	Return line of DHN
set	Threshold for the FC mode
sink	Sink of the VCC condenser
supply	Supply line of DHN
waste	Waste heat from DC at the condenser of VCC 1

References

1. European Union. European Directive 2023/1791. 2023. Available online: https://eur-lex.europa.eu/eli/dir/2023/1791/oj (accessed on: 30 January 2026).
2. Euroheat & Power. DHC MarketOutlook Insights &Trends. 2023. Available online: https://www.euroheat.org/data-insights/outlooks/market-outlook-2023 (accessed on: 30 January 2026).
3. International Energy Agency. Net Zero by 2050—A Roadmap for the Global Energy Sector. 2021. Available online: https://www.iea.org/reports/net-zero-by-2050 (accessed on 30 January 2026).
4. International Energy Agency. Net Zero Roadmap: A Global Pathway to Keep the 1.5 °C Goal in Reach. 2023. Available online: https://www.iea.org/reports/net-zero-roadmap-a-global-pathway-to-keep-the-15-c-goal-in-reach (accessed on: 30 January 2026).
5. International Renewable Energy Agency. World Energy Transitions Outlook 2023. 2023. Available online: https://www.irena.org/Publications/2023/Jun/World-Energy-Transitions-Outlook-2023 (accessed on: 30 January 2026).
6. Euroheat & Power. Large Heat Pumps in District Heating & Cooling Systems. 2022. Available online: https://www.euroheat.org/news/new-report-large-heat-pumps-in-district-heating-and-cooling-systems (accessed on: 30 January 2026).
7. International Energy Agency. *The Future of Heat Pumps*; OECD: Paris, France, 2022. https://doi.org/10.1787/2bd71107-en.
8. Werner, S. International review of district heating and cooling. *Energy* **2017**, *137*, 617–631. https://doi.org/10.1016/j.energy.2017.04.045.
9. Mazhar, A.R.; Liu, S.; Shukla, A. A state of art review on the district heating systems. *Renew. Sustain. Energy Rev.* **2018**, *96*, 420–439. https://doi.org/10.1016/j.rser.2018.08.005.
10. Lund, H.; Werner, S.; Wiltshire, R.; Svendsen, S.; Thorsen, J.E.; Hvelplund, F.; Mathiesen, B.V. 4th Generation District Heating (4GDH): Integrating smart thermal grids into future sustainable energy systems. *Energy* **2014**, *68*, 1–11. https://doi.org/10.1016/j.energy.2014.02.089.
11. Lund, H.; Østergaard, P.A.; Chang, M.; Werner, S.; Svendsen, S.; Sorknæs, P.; Thorsen, J.E.; Hvelplund, F.; Mortensen, B.O.G.; Mathiesen, B.V.; et al. The status of 4th generation district heating: Research and results. *Energy* **2018**, *164*, 147–159. https://doi.org/10.1016/j.energy.2018.08.206.
12. Köfinger, M.; Basciotti, D.; Schmidt, R.R.; Meissner, E.; Doczekal, C.; Giovannini, A. Low temperature district heating in Austria: Energetic, ecologic and economic comparison of four case studies. *Energy* **2016**, *110*, 95–104. https://doi.org/10.1016/j.energy.2015.12.103.

13. Ommen, T.; Thorsen, J.E.; Markussen, W.B.; Elmegaard, B. Performance of ultra low temperature district heating systems with utility plant and booster heat pumps. *Energy* **2017**, *137*, 544–555. https://doi.org/10.1016/j.energy.2017.05.165.
14. Ziemele, J.; Gravelsins, A.; Blumberga, A.; Blumberga, D. Combining energy efficiency at source and at consumer to reach 4th generation district heating: Economic and system dynamics analysis. *Energy* **2017**, *137*, 595–606. https://doi.org/10.1016/j.energy.2017.04.123.
15. Buffa, S.; Cozzini, M.; D'Antoni, M.; Baratieri, M.; Fedrizzi, R. 5th generation district heating and cooling systems: A review of existing cases in Europe. *Renew. Sustain. Energy Rev.* **2019**, *104*, 504–522. https://doi.org/10.1016/j.rser.2018.12.059.
16. Dang, L.M.; Nguyen, L.Q.; Nam, J.; Nguyen, T.N.; Lee, S.; Song, H.-K.; Moon, H. Fifth generation district heating and cooling: A comprehensive survey. *Energy Rep.* **2024**, *11*, 1723–1741. https://doi.org/10.1016/j.egyr.2024.01.037.
17. Guelpa, E.; Verda, V. Demand response and other demand side management techniques for district heating: A review. *Energy* **2021**, *219*, 119440. https://doi.org/10.1016/j.energy.2020.119440.
18. Capone, M.; Guelpa, E. Implementing Optimal Operation of Multi-Energy Districts with Thermal Demand Response. *Designs* **2023**, *7*, 11. https://doi.org/10.3390/designs7010011.
19. Martinazzoli, G.; Pasinelli, D.; Lezzi, A.M.; Pilotelli, M. Design of a 5th Generation District Heating Substation Prototype for a Real Case Study. *Sustainability* **2023**, *15*, 2972. https://doi.org/10.3390/su15042972.
20. Ebrahimi, K.; Jones, G.F.; Fleischer, A.S. A review of data center cooling technology, operating conditions and the corresponding low-grade waste heat recovery opportunities. *Renew. Sustain. Energy Rev.* **2014**, *31*, 622–638. https://doi.org/10.1016/j.rser.2013.12.007.
21. Capozzoli, A.; Primiceri, G. Cooling Systems in Data Centers: State of Art and Emerging Technologies. *Energy Procedia* **2015**, *83*, 484–493. https://doi.org/10.1016/j.egypro.2015.12.168.
22. Habibi Khalaj, A.; Halgamuge, S.K. A Review on efficient thermal management of air- and liquid-cooled data centers: From chip to the cooling system. *Appl. Energy* **2017**, *205*, 1165–1188. https://doi.org/10.1016/j.apenergy.2017.08.037.
23. Alkrush, A.A.; Salem, M.S.; Abdelrehim, O.; Hegazi, A.A. Data centers cooling: A critical review of techniques, challenges, and energy saving solutions. *Int. J. Refrig.* **2024**, *160*, 246–262. https://doi.org/10.1016/j.ijrefrig.2024.02.007.
24. Daraghmeh, H.M.; Wang, C.-C. A review of current status of free cooling in datacenters. *Appl. Therm. Eng.* **2017**, *114*, 1224–1239. https://doi.org/10.1016/j.applthermaleng.2016.10.093.
25. International Energy Agency. Energy and AI. 2025. Available online: https://www.iea.org/reports/energy-and-ai (accessed on 30 January 2026).
26. ABI Research. Data Center Energy Consumption Forecast, 2024–2030. 2025. Available online: https://www.abiresearch.com/blog/data-center-energy-consumption-forecast (accessed on 30 January 2026).
27. Gartner. Gartner Says Electricity Demand for Data Centers to Grow 16% in 2025 and Double by 2030. 2025. Available online: https://www.gartner.com/en/newsroom/press-releases/2025-11-17-gartner-says-electricity-demand-for-data-centers-to-grow-16-percent-in-2025-and-double-by-2030 (accessed on 30 January 2026).
28. Ni, J.; Jin, B.; Zhang, B.; Wang, X. Simulation of Thermal Distribution and Airflow for Efficient Energy Consumption in a Small Data Centers. *Sustainability* **2017**, *9*, 664. https://doi.org/10.3390/su9040664.
29. Oró, E.; Depoorter, V.; Garcia, A.; Salom, J. Energy efficiency and renewable energy integration in data centres. Strategies and modelling review. *Renew. Sustain. Energy Rev.* **2015**, *42*, 429–445. https://doi.org/10.1016/j.rser.2014.10.035.
30. Oró, E.; Depoorter, V.; Pflugradt, N.; Salom, J. Overview of direct air free cooling and thermal energy storage potential energy savings in data centres. *Appl. Therm. Eng.* **2015**, *85*, 100–110. https://doi.org/10.1016/j.applthermaleng.2015.03.001.
31. He, Z.; Ding, T.; Liu, Y.; Li, Z. Analysis of a district heating system using waste heat in a distributed cooling data center. *Appl. Therm. Eng.* **2018**, *141*, 1131–1140. https://doi.org/10.1016/j.applthermaleng.2018.06.036.
32. Yuan, X.; Liang, Y.; Hu, X.; Xu, Y.; Chen, Y.; Kosonen, R. Waste heat recoveries in data centers: A review. *Renew. Sustain. Energy Rev.* **2023**, *188*, 113777. https://doi.org/10.1016/j.rser.2023.113777.
33. Socci, L.; Rocchetti, A.; Verzino, A.; Zini, A.; Talluri, L. Enhancing third-generation district heating networks with data centre waste heat recovery: Analysis of a case study in Italy. *Energy* **2024**, *313*, 134013. https://doi.org/10.1016/j.energy.2024.134013.
34. Sorknæs, P.; Nielsen, S.; Lund, H.; Mathiesen, B.V.; Moreno, D.; Thellufsen, J.Z. The benefits of 4th generation district heating and energy efficient datacentres. *Energy* **2022**, *260*, 125215. https://doi.org/10.1016/j.energy.2022.125215.
35. Miškić, J.; Dorotić, H.; Pukšec, T.; Soldo, V.; Duić, N. Optimization of data centre waste heat integration into the low-temperature district heating networks. *Optim. Eng.* **2024**, *25*, 63–91. https://doi.org/10.1007/s11081-023-09837-5.

36. Wahlroos, M.; Pärssinen, M.; Manner, J.; Syri, S. Utilizing data center waste heat in district heating—Impacts on energy efficiency and prospects for low-temperature district heating networks. *Energy* **2017**, *140*, 1228–1238. https://doi.org/10.1016/j.energy.2017.08.078.
37. Jerez Monsalves, J.; Bergaentzlé, C.; Keles, D. Impacts of flexible-cooling and waste-heat recovery from data centres on energy systems: A Danish case study. *Energy* **2023**, *281*, 128112. https://doi.org/10.1016/j.energy.2023.128112.
38. Pärssinen, M.; Wahlroos, M.; Manner, J.; Syri, S. Waste heat from data centers: An investment analysis. *Sustain. Cities Soc.* **2019**, *44*, 428–444. https://doi.org/10.1016/j.scs.2018.10.023.
39. Davies, G.F.; Maidment, G.G.; Tozer, R.M. Using data centres for combined heating and cooling: An investigation for London. *Appl. Therm. Eng.* **2016**, *94*, 296–304. https://doi.org/10.1016/j.applthermaleng.2015.09.111.
40. Wu, D.; Hu, B.; Wang, R.Z. Vapor compression heat pumps with pure Low-GWP refrigerants. *Renew. Sustain. Energy Rev.* **2021**, *138*, 110571. https://doi.org/10.1016/j.rser.2020.110571.
41. Jiang, J.; Hu, B.; Wang, R.Z.; Deng, N.; Cao, F.; Wang, C.-C. A review and perspective on industry high-temperature heat pumps. *Renew. Sustain. Energy Rev.* **2022**, *161*, 112106. https://doi.org/10.1016/j.rser.2022.112106.
42. Zini, A.; Socci, L.; Vaccaro, G.; Rocchetti, A.; Talluri, L. Working Fluid Selection for High-Temperature Heat Pumps: A Comprehensive Evaluation. *Energies* **2024**, *17*, 1556. https://doi.org/10.3390/en17071556.
43. Lund, R.; Persson, U. Mapping of potential heat sources for heat pumps for district heating in Denmark. *Energy* **2016**, *110*, 129–138. https://doi.org/10.1016/j.energy.2015.12.127.
44. David, A.; Mathiesen, B.V.; Averfalk, H.; Werner, S.; Lund, H. Heat Roadmap Europe: Large-Scale Electric Heat Pumps in District Heating Systems. *Energies* **2017**, *10*, 578. https://doi.org/10.3390/en10040578.
45. Požgaj, D.; Pavković, B.; Delač, B.; Glažar, V. Retrofitting of the District Heating System Based on the Application of Heat Pumps Operating with Natural Refrigerants. *Energies* **2023**, *16*, 1928. https://doi.org/10.3390/en16041928.
46. Chicherin, S.; Zhuikov, A.; Junussova, L. Integrating a heat pump into a 4th generation district heating (4GDH) system—Two-mode configuration inputting operational data. *Energy Build.* **2022**, *275*, 112445. https://doi.org/10.1016/j.enbuild.2022.112445.
47. Østergaard, P.A.; Andersen, A.N. Economic feasibility of booster heat pumps in heat pump-based district heating systems. *Energy* **2018**, *155*, 921–929. https://doi.org/10.1016/j.energy.2018.05.076.
48. Yang, X.; Svendsen, S. Ultra-low temperature district heating system with central heat pump and local boosters for low-heat-density area: Analyses on a real case in Denmark. *Energy* **2018**, *159*, 243–251. https://doi.org/10.1016/j.energy.2018.06.068.
49. Sarbu, I.; Sebarchievici, C. A Comprehensive Review of Thermal Energy Storage. *Sustainability* **2018**, *10*, 191. https://doi.org/10.3390/su10010191.
50. Scapino, L.; Zondag, H.A.; Van Bael, J.; Diriken, J.; Rindt, C.C.M. Sorption heat storage for long-term low-temperature applications: A review on the advancements at material and prototype scale. *Appl. Energy* **2017**, *190*, 920–948. https://doi.org/10.1016/j.apenergy.2016.12.148.
51. Airò Farulla, G.; Cellura, M.; Guarino, F.; Ferraro, M. A Review of Thermochemical Energy Storage Systems for Power Grid Support. *Appl. Sci.* **2020**, *10*, 3142. https://doi.org/10.3390/app10093142.
52. Gbenou, T.; Fopah-Lele, A.; Wang, K. Recent Status and Prospects on Thermochemical Heat Storage Processes and Applications. *Entropy* **2021**, *23*, 953. https://doi.org/10.3390/e23080953.
53. Guelpa, E.; Verda, V. Thermal energy storage in district heating and cooling systems: A review. *Appl. Energy* **2019**, *252*, 113474. https://doi.org/10.1016/j.apenergy.2019.113474.
54. Roger-Lund, S.; Darkwa, J.; Worall, M.; Calautit, J.; Boukhanouf, R. A Review of Thermochemical Energy Storage Systems for District Heating in the UK. *Energies* **2024**, *17*, 3389. https://doi.org/10.3390/en17143389.
55. Capone, M.; Guelpa, E.; Mancò, G.; Verda, V. Integration of storage and thermal demand response to unlock flexibility in district multi-energy systems. *Energy* **2021**, *237*, 121601. https://doi.org/10.1016/j.energy.2021.121601.
56. Böhm, H.; Lindorfer, J. Techno-economic assessment of seasonal heat storage in district heating with thermochemical materials. *Energy* **2019**, *179*, 1246–1264. https://doi.org/10.1016/j.energy.2019.04.177.
57. THUNDER Horizon Project Consortium. THermochemical storage Utilization eNabling Data centre seasonal Energy Recovery. Available online: https://www.thunderproject.eu (accessed on 30 January 2026).
58. ASHRAE TC 9.9. 2021 Equipment Thermal Guidelines for Data Processing Environments. 2021. Available online: https://www.ashrae.org/file%20library/technical%20resources/bookstore/supplemental%20files/therm-gdlns-5th-r-e-ref-card.pdf (accessed on 30 January 2026).
59. Musilli, J.; Ellison, B. Facilities Design for High-density Data Centers. 2012. Available online: https://www.intel.cn/content/dam/www/public/us/en/documents/best-practices/data-center-facilities-paper.pdf (accessed on 30 January 2026).

60. SolarTech. How Much Electricity Does a Data Center Use? Complete 2025 Analysis. IAEI Magazine. 2026. Available online: https://iaeimagazine.org/electrical-fundamentals/how-much-electricity-does-a-data-center-use-complete-2025-analysis/ (accessed on 30 January 2026).
61. Danfoss. CoolSelector. Available online: https://www.danfoss.com/it-it/service-and-support/downloads/dcs/coolselector-2/ (accessed on 30 January 2026).
62. Rocchetti, A.; Socci, L. Study of a novel Humidification-Dehumidification Desalination system hybridised with Indirect Evaporative Cooling and Vapour Compression Refrigeration. *Therm. Sci. Eng. Prog.* **2025**, *61*, 103513. https://doi.org/10.1016/j.tsep.2025.103513.
63. *Manuale Degli Impianti di Climatizzazione*; Tecniche Nuove: Milan, Italy, 2008; ISBN 978-88-481-1884-2
64. Arpagaus, C.; Bless, F.; Uhlmann, M.; Schiffmann, J.; Bertsch, S.S. High temperature heat pumps: Market overview, state of the art, research status, refrigerants, and application potentials. *Energy* **2018**, *152*, 985–1010. https://doi.org/10.1016/j.energy.2018.03.166.

Disclaimer/Publisher's Note: The statements, opinions and data contained in all publications are solely those of the individual author(s) and contributor(s) and not of MDPI and/or the editor(s). MDPI and/or the editor(s) disclaim responsibility for any injury to people or property resulting from any ideas, methods, instructions or products referred to in the content.